Computation Simulation of Empty Fruit Bunch Biomass Combustion in a Water-Tube Boiler

Peter Chin Jie Vui[1] Arshad Adam Salema[*,2] Farid Nasir Ani[1]

[1]*School of Mechanical Engineering, Faculty of Engineering, Universiti Teknologi Malaysia, 81310 UTM Johor Bahru, Johor Bahru, Malaysia.*
[2]*School of Engineering, Monash University Malaysia, Jalan Lagoon Selatan, Bandar Sunway 47500, Selangor, Malaysia.*
**Corresponding author. E-mail: arshad.salema@monash.edu*

ABSTRACT
This study aims to reduce NOx emission by optimizing the secondary air system of the boiler using computational modeling and simulation. The shredded EFB is introduced in the inclined bed with primary air supply from the bottom of the bed. FLUENT Ver. 15.0 computational software is used to simulate the combustion of EFB in the grate-fired boiler and investigate the effect of four secondary air arrangements on the combustion characteristic and NOx emission level. The secondary air stream was optimized using an internal flue gas circulation system. Each case was compared to the initial setting. Results suggested that a tangential arrangement of the secondary air system promotes a better mixing rate and higher residence time, giving a lower combustion peak temperature of 1853 K which leads to a lower NOx emission of 257 ppm.

Keywords: *Empty fruit bunch, Biomass, Simulation, Boiler, Emission*

1. INTRODUCTION

Steam boiler systems are in fact integrated into almost all the major industrial processes for both heat and power. Most of the industries heavily rely on fossil fuels as a source of energy for the boiler system. However, this comes with the expense of fuel prices and emissions. The environmental impact of greenhouse gases (GHG) generating from the combustion of fossil fuels has led to climate change (global warming), acidic gases that damage both structural and human health. The main concern is to minimize the emission from the combustion process/technologies while maintaining, or even increasing the thermal efficiency of the process [1]. The increase in the efficiency of a steam boiler will improve the viability of heat/power generation. Therefore, there is a high motivation for alternatives and renewable energy sources that are clean and sustainable.

One such renewable source of energy is biomass. For instance, in Malaysia and surrounding countries, oil palm mill generates millions of tons of biomass per year in form of empty fruit bunch (EFB), oil palm shell (OPS), oil palm fiber (OPF), palm fronds, and oil palm trunk [1]. Oil palm mill utilizes EFB and OPS to some extent as an alternative fuel to provide heat and power to the oil palm mills and refineries using a biomass grate-fired boiler.

Grate-fired boilers typically can adapt to fuels of varying calorific value and moisture content has high carbon-in ash, low efficiency and high emissions [1]. The modern design of a grate-fire boiler has 4 main parts; namely the grate, air supply system (primary and secondary), fuel supply system, and ash and exhaust discharge system. Although the grate fire boiler has great potential in biomass combustion, according to Fazeli [2], there are still challenges related to the reaction in the fuel bed region, solid and gaseous combustion, char formation, pollutant emission, and ash deposition. The most notable pollutant found in a biomass boiler is the NOx compounds. This arises mainly due to the fuel-bound nitrogen found in most of the biomass fuel. During a combustion process, this fuel-bound nitrogen is released in the form of NO, NH3, HCN species [3]. The direct formation of NO emission is also caused due to the O/N ratio in biomass [4]. Therefore, it is necessary to investigate the combustion behavior as well as the emissions from the boiler. This study is directed toward emission control specifically, the NOx.

The combustion performance of the grate boiler can be greatly improved by optimizing the primary and secondary air distribution beneath the grate, promoting mixing efficiency, and reducing the probability of air leakage from the combustion chamber [5]. Among these secondary air plays an important role in complete combustion of biomass particles specifically in the freeboard region of the boiler [5].

It is difficult and expensive to carry out comprehensive experimental studies on grate-fired boilers to observe the parameters and combustion behavior affecting the boiler's performance. However, numerical modeling and CFD simulation [5, 6-10] can help to visualize and understand

the problem of combustion and optimize the plant operation by modifying the plant design. Modeling and simulation of the combustion in the fuel bed are important to understand the release and formation of NOx. While modeling the combustion in the freeboard will help to optimize the mixing behavior to improve the burnout rate and lower the emissions [5].

1.1. Related Work

Most literature on combustion CFD modeling focuses on optimizing the mixing process. The problem with poor mixing the grate fired boiler can arise from low retention time which results in insufficient mixing between the secondary air and the volatiles bulk flow; or highly heterogeneous distribution of flue gas and flame front within the voile of the combustion chamber, or high channeling flow between the freeboard and exhaust outlet [11].

A 3D Eddy Break-up model (EBU), a turbulence mixing controlled combustion model was used to investigate the combustion phenomenon of woody biomass fuels in a reciprocating grate furnace [12]. They concluded that the combustion of biomass in a grate furnace can provide improved burnout and higher temperature with a proper O2/CO2 ratio.

Very recently, a new physical solution under a comprehensive Eulerian model that tackles the complex problem of biomass movements inside a packed boiler bed was developed by [13]. Their model responded well, in most of the real cases, however, exhibited good performance when recreating the physics of the bed integrated with ANSYS Fluent solver.

The objective of [14] was to numerically investigate the impact of the grate inlet conditions at the top surface of the fuel bed on the CFD simulation of the flow, combustion and heat transfer in the freeboard of a waste wood-fired grate boiler. They found that after the addition of the secondary combustion chamber, the CFD results based on different fuel bed models were close to each other.

A good agreement between the modeling and simulation results from the coupled model and the on-site measurement data from a wood-chip grate boiler for steam generation, was achieved [15]. In another study [16], a numerical modeling method was developed to simulate the whole combustion process of biomass in a grate firing boiler to reduce the NOx formation. For this, they developed internal flue gas recirculation technology (IFGRT) to mitigate the NO formation in the grate boiler through thermal, NNH and N2O routes. Further, they [17] even used the Fluent model to simulate the NOx formation during the co-combustion of biomass with methane.

1.2. Our Contribution

The main objective of this study was to simulate the combustion behavior in order to reduce the NOx emission in a grate-fired boiler. The first part of the study is focused on detailed modeling of the solid biomass fuel reaction which involves mass conversion, heat transfer and bulk volume changing and mass dispersion. The main interest in the modeling is to study the flame front, in which the propagation determines the de-volatilization process and governs the overall heat radiation to both the grate area and the freeboard region. The propagation of the flame front also dictates most of the fuel-bound pollutant emission, for example, particulate matters, NOx, SOx, and etc.

2. METHODOLOGY

Biomass fuel comprises varying moisture content, particle shapes, sizes, volatile matter content and a smaller amount of nitrogen (N) and Sulphur (S) compared to coal. By using the basis of a coal calculator built-in function in Fluent, the physical and chemical fuel properties of EFB biomass can be modeled numerically. The fuel properties that are required for the calculation are the material bulk density of fuel, fuel composition from both ultimate and proximate analysis, pyrolysis yield, porosity for bed and fuel, dimension and shape of fuel particle, effective thermal conductivity, effective mass dispersion coefficient, dynamic viscosity, emissivity, and specific heat capacities of gas and fuel.

Figure 3.1 shows the modeling flow chart of the project, in which Gratecal numerical for the fuel bed model is needed to generate the boundary conditions for the input into the freeboard model in FLUENT. Gratecal basically solves the Navier-Stokes PDE and pressure drop equations. The following are the assumptions adopted to model the fuel bed as a 2D numerical model:

- The fuel bed is considered as a continuous domain with homogeneous porosity distributed evenly across the grid that consisting both gas and solid phases.
- The fuel particles are assumed to be thin, there zero pressure gradient across the particle thickness.
- The solid fuels are assumed to comprise only 4 species, which are volatiles, char, ash, and moisture.
- Within the fuel bed, the reaction can be divided into 4 sub-processes: drying (evaporation of moisture), de-volatilization and char formation, oxidation of volatiles, and char burnout.
- All gases are assumed to be incompressible and behave like an ideal gas, plug flow is adopted.
- The solid is assumed to move horizontally, there are no solid particles carried upward by the primary airflow.
- Pressure drop is calculated based on the homogeneous viscosity distribution of the air in both x and y-direction.
- The volatile gas released consist of species limited to H2O, O2, CO, CO2, H2, N2, CH4, CXHYOZ.
- The radiated heat within the bed is modeled based on the effective thermal conductivity.

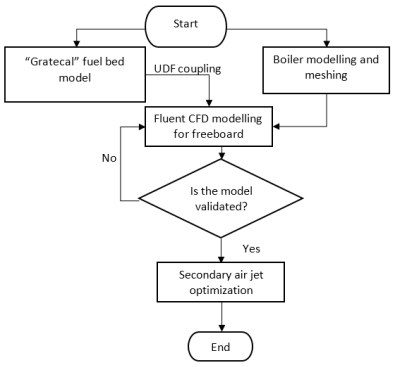

Figure 1 Modeling and simulation flowchart

When combustion propagates within the solid fuel bed, gaseous volatiles is released from the bed and enter the freeboard, for which the species concentrations, mass flux and temperature must be supplied as inlet boundary conditions to the freeboard reaction. For grate combustion modeling, there is a strong coupling between processes occurring inside the fuel bed and in the freeboard region; inappropriate treatment of the boundary conditions may lead to inaccurate results of a simulation, mainly in the vicinity of the fuel bed [18, 19]. A MATLAB based fuel bed numerical code is adopted to simulate the bed reaction. Figure 2 shows the boundary conditions of the 2D bed model.

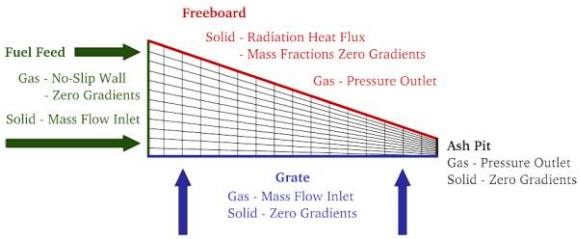

Figure 2 Fuel bed model boundary conditions

On the fuel bed, the fuel feeding rate, the primary air rate, and the result from proximate analysis and ultimate analysis is defined as the boundary conditions for the bed model. The bed model in turn generates species concentrations, temperature and mass flux and input into the freeboard model. As the top of the fuel layer is heated up by radiation from hot gases in the freeboard, the radiation must be considered in the boundary condition for the bed condition. Both fuel bed and freeboard model are coupled by a C library UDF code. The following equations are model included in fuel bed model:

Bed porosity shrinkage:

$$\phi = \phi_0 + (1-\phi_0)\sum_t f_t(X_{t,0} - X_t) \quad (1)$$

Fuel Particles surface area:

$$A_p = \frac{4(1-\phi_b)d_{out}}{d_{out}^2 - d_{in}^2} \quad (2)$$

Gas phase energy conservation:

$$\frac{\partial(\phi\rho_g Y_{ig})}{\partial t} + \frac{\partial(\phi\rho_g V_g Y_{ig})}{\partial x} = \frac{\partial}{\partial x}\left[\lambda_g \frac{\partial T_g}{\partial x}\right] + S_a h_s'(T_s - T_g) + Q_h \quad (3)$$

$$\lambda_g = 2.27\cdot 10^{-7}\left(\frac{d_p}{1-\epsilon_b}\right)\left(\frac{\epsilon_{rad,p_b}}{2-\epsilon_b}\right)T_s^3 \quad (4)$$

Solid phase energy conservation:

$$\frac{\partial((1-\phi)\rho_p H_s)}{\partial t} + \frac{\partial((1-\phi)\rho_p V_s H_s)}{\partial x} = \frac{\partial}{\partial x}\left[\lambda_s \frac{\partial T_s}{\partial x}\right] + S_a h_s'(T_g - T_s) + \frac{\partial q_r}{\partial x} + Q_{sh} \quad (5)$$

$$\lambda_s = \left(\frac{\rho_s}{4511}\right)^{3.5} T_s^{0.5} + 2.27\cdot 10^{-7}\left(\frac{d_p}{1-\epsilon_b}\right)\left(\frac{\epsilon_{rad,p_b}}{2-\epsilon_b}\right)T_s^3 \quad (6)$$

Specific heat capacity of gas and fuel:

$$c_{p,g}(T_s) = 990 + 0.122T_g - 5680\cdot 10^3 T_g^{-2} \quad (7)$$

Pressure drop across bed:

$$\frac{\Delta p d_p^2 \epsilon_b^3}{L\mu v(1-\epsilon_b)^2} = \left(3.81 - \frac{5.265}{\left(\frac{d_t}{d_{p,e}}\right)} - \frac{7.047}{\left(\frac{d_t}{d_{p,e}}\right)^2}\right)\frac{\rho_g v d_p}{\mu(1-\epsilon_b)} + 211 \quad (8)$$

The boiler design is shown in Figure 3, in which the simulation domain is highlighted with a black line. The diagram shows the original design with a parallel secondary air injection as circled in red. This work focus on the study of the effect of changing the arrangement of the secondary air jet on the initial horizontal plane. Internal flue gas circulation is also included in these cases to study the feasibility of implementing the technology. Table 1 summarizes the freeboard model adopted in this work.

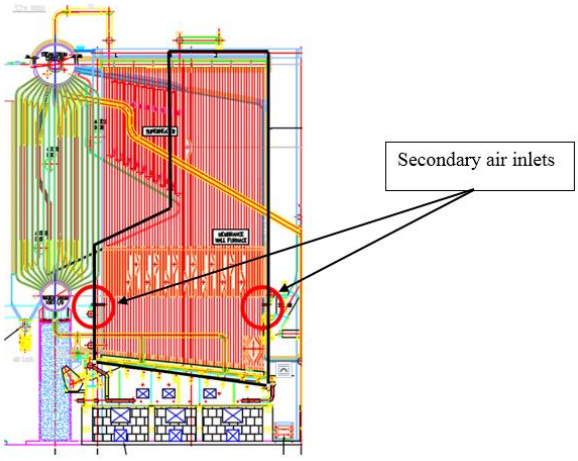

Figure 3 Boiler design and simulation domain

The fuel conversion took place in the fuel bed boiler grate and homogenous gaseous combustion in the upper freeboard of the boiler. The volatiles released during the combustion process of the biomass can be represented by the empirical formula C1.53H2.43O, and the detail of the composition is listed in Table 2. Species wise, the combustible mixture is majorly comprised of CH4, CO, H2 and $C_xH_yO_z$. The species details are extracted from the bed model and input into FLUENT and up 20 intermediate species are considered in generating the non-premixed combustion PDF table. Realizable κ-ε model is chosen to solve flow turbulence, the discrete ordinate (DO) model is chosen to simulate the radiation heat transfer between gases and furnace walls, and the assumption weighted sum of grey gas (WSGG) is taken to estimate the absorption coefficient of the PDF mixture.

Table 1 Fluent model used in the simulation work

Parameter	**Model**
Space	3D Cartesian
Mesh	751866 cells
Fluid mechanics	Continuity equation Model
Turbulent	Realized k-e Model with standard wall function
Heat	Energy equation Model
Radiation Model	Discrete Ordinates (DO) with WSGG
Species Transport	Non-Premixed Combustion by PDF mixture with the adoption of inlet diffusion
Reactions model	Eddy Dissipation (EDS)
Pollutant	Thermal NOx with reduction model, Fuel NOx, Prompt NOx, GRI 3.0 reaction mechanism
Boundary Condition	**Value**
Fuel feeding rate	10,000 kg/hr
Total volatile rate	0.9477 kg/s
Primary air rate	5.16 kg/s
Secondary air rate	1.57 kg/s

Table 2 Chemical properties of EFB biomass

Proximate analysis (wt%)		**Element analysis (wt%)**	
Fixed carbon	10.78	C	49.38
Volatiles matter	75.91	H	6.52
Moisture	7.95	O	42.90
Ash	5.36	N	0.7
HCV (MJ/lg)	19.4	S	0.5

Figure 4 shows a detailed illustration of the different secondary air supply system studied in this research project. The boiler was initially designed with a parallel secondary air injection system with 2 pairs of nozzles spread across the furnace wall. In this study, only the injection arrangement was changed while maintaining the total mass flux of the secondary air constant throughout the cases. The one-sided case is to check whether reducing the nozzles amount and maintaining the same mass flux would increase the air injection velocity. This will lead to a higher turbulent flow on the flame front. The staggered and tangential arrangement would give a similar value of the injection velocity to the one-sided arrangement, but the orientation is arranged in such a way that it provides more turbulent flow due to vortices.

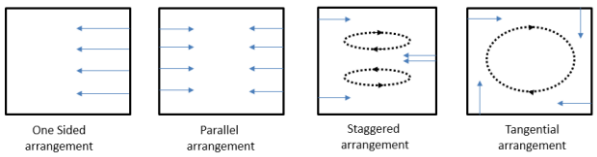

Figure 4 Different case studies schematic illustration of secondary air injection in the freeboard region

3. RESULTS AND DISCUSSION

3.1. Model validation

The validation is done on the base model by comparing the numerical result against the onsite (real-time) reading of temperature and mass flux at the exhaust toward the superheated tube in the boiler. Table 3 shows the comparison results of both temperature and mass flux between the onsite measurements and numerical prediction. The error percentages are small which means the numerical result is very close to the measured data on-site. The model is accepted and validated with 15% error tolerance. Therefore, the present modeling approach will be continued and adapted to the study cases. For instance, the difference between calculated and measured for O_2, CO and gas temperature was 5.9%, 20.4% and 5.8%, respectively [7]. In their study and others [8], the calculated or predicted values were higher than measured or experimental values.

Table 3 Comparison of measured and predicted values of the base case

Parameters	**Measured (average)**	**Predicted**
Temperature, K	1097	1146
Velocity, m/s	5.12	4.68

3.2. Flow properties

Figure 5 shows the velocity vector (flow profile) of secondary air injection that is located at the nozzle plane among the studied cases (Figure 4). Under the parallel arrangement, velocity is relatively low, no apparent vortices can be deduced from the flow field. The one-sided arrangement gives a much stronger flow, in which the flame front is switched more toward the nozzle for lean combustion. As for the staggered and tangential cases, apparent vortices can be seen in the flow field where the internal flue gas circulation occurs right above the flame front. The tangential arrangement created a hurricane-like flow connecting the flame front to the exhaust outlet, which later will be further discussed in terms of temperature profile and the NOx emission comparison. The overall effect of the secondary air is that it creates a recirculation zone that pushes the air downward [7]. This internal circulation is important to generate strong turbulence and mixing between the volatile gas released from biomass and air injected in the freeboard region [11]. Tu et al. [16] also observed a recirculation zone separated into two parts in a staggered arrangement which agrees with the present study.

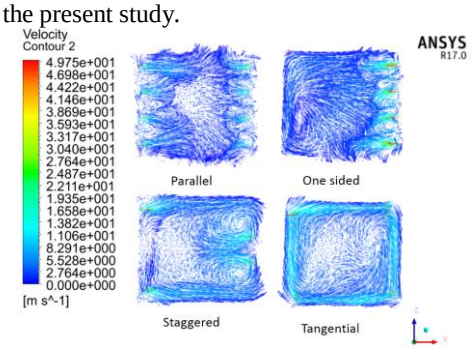

Figure 5 Velocity profile of different cases on the secondary air nozzle plane

3.3 Combustion characteristics

By recirculating the internal flue gas through the secondary air injection nozzle, a significant impact on the combustion properties in the freeboard region can be observed. As shown in Figure 7, the maximum temperature was at around 1700 to 1800 K. The overall flame kernel (size) decreased in one-sided, staggered and tangential cases compared to the original parallel arrangement. The temperature dropped in all these three cases, while the drop was more obvious in the staggered and tangential arrangement. This is due to a decrease in the flame kernel size [16]. The temperature was more evenly spread out in the tangential arrangement case (Figure 6) due to the circular velocity profile of the air. The good mixing by the secondary air and the burnout in the secondary combustion makes the temperature more evenly in the freeboard region [14]. The boiler tube membrane walls were exposed to the green temperature zone (around 1061 K). Therefore, the tangential arrangement can provide more consistent temperature control in the boiler furnace than in other cases.

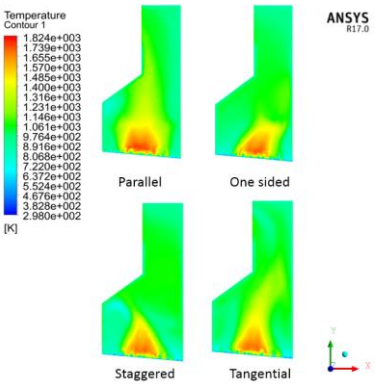

Figure 6 Temperature profile of different cases on the mid-plane of the furnace

3.4 Comparison of NO emission

Figure 7 shows the distribution of NO inside the furnace for all the cases. The maximum NO concentration is estimated at 1114 ppm for the original parallel setting at the flame front, whereas the concentration is 600 ppm at the exhaust. For the one-sided and staggered case, the maximum concentration is at 771 ppm at the flame front and the average concentration is at 342 ppm at the exhaust. The best result is the tangential case, in which the maximum concentration is 428ppm and the average at the exhaust is 257 ppm.

NO is more concentrated near the grate bed is mainly derived from fuel-bound nitrogen. The reduction of NO can be observed in all the 3 cases that agree with the previous study [16]. The most notable is from the tangential arrangement case, which has the highest mixing rate and residence time, suppressing the NOx formation and promoting destruction mechanism, hence giving it the lowest pollutant concentration.

Apart from the fuel NOx formation route, thermal NOx formation (N + OH→H + NO; N2 + O→N + NO) is another way that contributes to the emission of NOx, which can be observed from Figure 6 and Figure 7 that the NOx pollutant profile shares the same shape with the temperature profile of the 3 study cases. With a relatively lower temperature in the study cases, where the temperature is not high enough to severe the N-N covalent bond, the thermal NOx formation was inhibited, thus, greatly reduce the concentration. By recirculating the internal flue gas, it can be observed that the mean temperature of the combustion remains while the maximum temperature decreases, where the temperature profile has an overall similar green patch but with different maximum temperatures near the flame front.

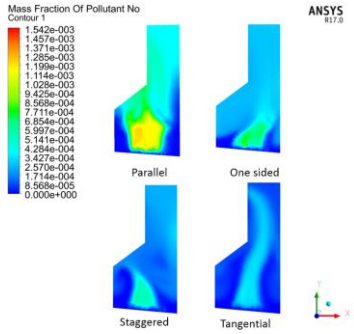

Figure 7 NO pollutant mass fraction contour of the study cases on the middle plane of the furnace

The oxygen radical formation is suppressed and leads to a suppression to the prompt NO (N + OH→H + NO; N2 + O→N + NO) and N2O (NCO + OH→NO + H + CO; NCO + O2→NO + CO2) formation mechanism [11]. Last but not least, as mention before, the trace amount of NO in the flue gas was recirculated into the freeboard instead of releasing into the exhaust, this promotes the re-burning process of NO to form N2 (NCO + NO→N2 + CO2; NH + NO→N2 +OH). Therefore, the whole process of NO reduction by using internal flue gas circulation is based on both the formation and destruction mechanisms.

As shown in Table 4, as a comparison to the result published [10], the predicated NOx emission has concentrated on the flame kernel right above the fuel bed, and from his study case, the staggered orientation did have an improvement in controlling the NOx emission, the concentration at the furnace exhaust is 292 ppm for the staggered cases. Other than that, according to National Air Standard, the NOx limit for a boiler with a power rating 14 MW and above is 0.4644 g/kWh. By assuming NO2 as the major components of NOx, the equivalent mass limit for a 15 MW boiler is around 7000 g/hr. From the previous discussion, the NOx emission predicted by the model is at 257 ppm, the equivalent mass is equal to 1735 g/hr, and therefore the predicted simulation result remains under the emission limit.

Table 4 Comparison of boiler NOx emission limit.

US boiler NOx emission limit	7000 g/hr
Tu et. al.	1971 g/hr
Present work	1735 g/hr

3. CONCLUSIONS

By using the fuel bed code and UDF for the coupling model in FLUENT to simulate the bed reaction of EFB biomass fuel, the temperature distribution, velocity profile, and volatiles species concentration can be predicted accurately and carry forward to the freeboard reaction simulation. The overall summary of models is by reducing the number of secondary air nozzles while maintaining the same mass flux to increased injection momentum and run a trial with different arrangements to generate different flow fields to study the effect of turbulent vortices. As a summary of the combustion characteristic, the maximum temperature is at around 1700 to 1800 K over 4 cases. The overall flame kernel (size) decreases with the 3 study cases compares to the original parallel arrangement. The tangential case shows the most homogeneous flame distribution across the boiler water-tube membrane walls. Furthermore, with the implementation of the internal flue gas circulation technology, all 3 study case arrangements succeed in suppressing maximum temperature reduce the overall flame size, and leading to a reduction of NO emission at 257ppm. Out of all, the tangential arrangement shows the most potential in the study and the arrangement should be implementing in the onsite boiler to verify the numerical result.

Nomenclature

ϕ_0	Initial bed porosity
$X_{i,0}$	Initial mass fraction of the i-th solid component
f_i	Shrinkage factor
d	Particle diameter
H_g	Gas enthalpy
Q_h	Heat gain of the gas phase due to combustion
λ_g	Thermal dispersion coefficient
Q_{sh}	Heat generation due to heterogeneous combustion
H_s	Solid-phase enthalpy
λ_s	Effective thermal conductivity of the solid bed
q_r	Radiative heat flux.
T_s	Solid phase temperature
d_p	Solid particle diameter
$\epsilon_{rad,p}$	Solid particle emissivity
$c_{p,s}$	Steffan-Boltzman constant
D_s	Particle diffusion coefficient

ACKNOWLEDGMENT

The author acknowledges the full supported by the Faculty of Mechanical Engineering, Universiti Teknologi Malaysia.

REFERENCES

[1] M.C. Barma, R. Saidur, S.M.A. Rahman, A. Allouhi, B.A. Akash, and S.M. Sait, A review on boilers energy use, energy savings, and emissions reductions, Renew. Sust. Energ. Rev. 79 (2017) 970–983. DOI: https://doi.org/10.1016/j.rser.2017.05.187

[2] A. Fazeli, B. Farzaneh, J. Leila, C.S. Nor Azwadi, and B.E. Ali, Malaysia′ s stand on municipal solid waste conversion to energy: A review. Renew. Sust. Energy Rev. 58 (2016) 1007-1016. DOI: https://doi.org/10.1016/j.rser.2015.12.270

[3] W. Blasiak, W.H. Yang, and W. Dong, Combustion performance improvement of grate fired furnaces using Ecotube system, J. Energy. Inst. 79(2) (2006) 67-74. DOI: https://doi.org/10.1179/174602206X103530

[4] H. Im, R. Firooz, and H. Mohammad, Formation of nitric oxide during tobacco oxidation, J. Agr. Food

Chem. 51(25) (2003) 7366-7372. DOI: https://doi.org/10.1021/jf030393w

[5] C. Yin, L.A. Rosendahl, and K.K. Søren, Grate-firing of biomass for heat and power production, Prog. Energy Combust. Sci. 34(6) (2008) 725-754. DOI: https://doi.org/10.1016/j.pecs.2008.05.002

[6] C. Li, D. Zhenghua, S. Zhonghua and W. Fuchen, Modeling of an opposed multiburner gasifier with a reduced-order model, Ind. Eng. Chem. Res. 52(16) (2013) 5825-5834. DOI: https://doi.org/10.1021/ie3030505

[7] A. Rezeau, I.D. Luis, R. Javier, and D-R. Maryori, Efficient diagnosis of grate-fired biomass boilers by a simplified CFD-based approach, Fuel Process Technol. 171 (2018) 318-329. DOI: https://doi.org/10.1016/j.fuproc.2017.11.024

[8] C.A. Bermúdez, J. Porteiro, L.G. Varela, S. Chapela, and D. Patiño, Three-dimensional CFD simulation of a large-scale grate-fired biomass furnace, Fuel Process Technol. 198 (2020) 106219. DOI: https://doi.org/10.1016/j.fuproc.2019.106219

[9] S. Zahirović, R. Scharler, P. Kilpinen, and I. Obernberger, Validation of flow simulation and gas combustion sub-models for the CFD-based prediction of NOx formation in biomass grate furnaces, Combust. Theor. Model 15(1) (2010) 61-87. DOI: https://doi.org/10.1080/13647830.2010.524312

[10] R. Boštjan, C. Yin, N. Samec, M. Hriberšek, F. Kokalj, and M. Zadravec, Advanced CFD modeling of air and recycled flue gas staging in a waste wood-fired grate boiler for higher combustion efficiency and greater environmental benefits, J. Environ. Manage. 218 (2018) 200-208. DOI: https://doi.org/10.1016/j.jenvman.2018.04.030

[11] S. João, J.Teixeira, S. Teixeira, S. Preziati, and J. Cassiano, CFD modeling of combustion in biomass furnace, Energy Procedia 120 (2017) 665-672. DOI: https://doi.org/10.1016/j.egypro.2017.07.179

[12] K. Md Rezwanul, A.A. Bhuiyan, and J. Naser, CFD simulation of biomass thermal conversion under air/oxy-fuel conditions in a reciprocating grate boiler, Renew. Energy 146 (2020) 1416-1428. DOI: https://doi.org/10.1016/j.renene.2019.07.068

[13] L.G. Varela, M.A. Gómez, M. Garabatos, D. Glez-Peña, and J. Porteiro, Improving the Bed Movement Physics of Inclined Grate Biomass CFD Simulations, Appl. Therm. Eng. 182 (2021) 116043. DOI: https://doi.org/10.1016/j.applthermaleng.2020.116043

[14] T. Zadravec, C. Yin, F. Kokalj, N. Samec, and B. Rajh, The impacts of different profiles of the grate inlet conditions on freeboard CFD in a waste wood-fired grate boiler, Appl. Energy 268 (2020): 115055. DOI: https://doi.org/10.1016/j.apenergy.2020.115055

[15] A. Zhou, H. Xu, W. Yang, Y. Tu, M. Xu, W. Yu, S.K. Boon, and P. Subbaiah, Numerical study of biomass grate boiler with coupled time-dependent fuel bed model and computational fluid dynamics based freeboard model, Energy Fuel 32(9) (2018) 9493-9505. DOI: https://doi.org/10.1021/acs.energyfuels.8b01823

[16] Y. Tu, A. Zhou, M. Xu, W. Yang, K. B. Siah, and P. Subbaiah, NOX reduction in a 40 t/h biomass fired grate boiler using internal flue gas recirculation technology, Appl. Energy 220 (2018) 962-973. DOI: https://doi.org/10.1016/j.apenergy.2017.12.018

[17] A. Zhou, H. Xu, M. Xu, W. Yu, Z. Li, and W. Yang, Numerical investigation of biomass co-combustion with methane for NOx reduction, Energy 194 (2020) 116868. DOI: https://doi.org/10.1016/j.energy.2019.116868

[18] M. Costa, N. Massarotti, V. Indrizzi, B. Rajh, C. Yin, and N. Samec, Engineering bed models for solid fuel conversion process in grate-fired boilers, Energy, 77 (2014) 244-253. DOI: https://doi.org/10.1016/j.energy.2014.07.067

[19] A. Kraszkiewicz, A. Przywara, M. Kachel-Jakubowska, and E. Lorencowicz, Combustion of Plant Biomass Pellets on the Grate of a Low Power Boiler, Agric. Agric. Sci. Procedia, 7 (2015) 131-138. DOI: https://doi.org/10.1016/j.aaspro.2015.12.007